Induced Circular Dichroism of β-Cyclodextrin Complexes with *o*-, *m*-, and *p*-Disubstituted Benzenes

Hiroshi Shimizu, Akira Kaito,† and Masahiro Hatano*

Chemical Research Institute of Non-aqueous Solutions, Tohoku University, Katahira, Sendai 980

(Received April 23, 1980)

The induced circular dichroism (ICD) spectra of β-cyclodextrin (β-$\mathrm{CD_x}$) complexes with *o*-, *m*-, and *p*-disubstituted benzenes were observed. The comparison of the observed rotational strengths with the ones calculated by using the Kirkwood-Tinoco expression is examined; the possible orientations of the guest molecules which are included in the cavity of β-$\mathrm{CD_x}$ are presented. These results suggest that the orientation of the guest molecule is confined about the axis of the β-$\mathrm{CD_x}$ torus.

The cyclodextrins ($\mathrm{CD_x}$'s) are α-1,4 linked oligomers of D-glucose formed during the degradation of starch by an amylase of *Bacillus macerans*, and have 6, 7, or 8 glucose residues per molecule.[1] It is known that $\mathrm{CD_x}$ can include aromatic compounds, alkyl halides, and gases, as guest molecules in its cavity, resulting in the formation of inclusion complexes.[2] This characteristic has led to their utilization as enzyme models.[3-6] In recent years, many extensive investigations on the suitability of modified $\mathrm{CD_x}$ or capped $\mathrm{CD_x}$ as a enzyme model have been carried out.[7-9]

The orientation of the guest molecule which is included in the cavity of $\mathrm{CD_x}$ plays an important role in the inclusion phenomenon. More information on the structure of the $\mathrm{CD_x}$ complex with mono- or disubstituted benzene will be very significant, since substituted benzenes are sometimes used as substrates of the reactions catalyzed by $\mathrm{CD_x}$'s.

The circular dichroism (CD) study is one of the most useful physico-chemical methods for elucidating the orientation of the guest molecule included by $\mathrm{CD_x}$ in solution. That is to say, the CD is expected to be induced at the absorption bands of the achiral guest molecules which are included in the cavity of the chiral $\mathrm{CD_x}$ host molecule, since $\mathrm{CD_x}$ is composed of chiral glucose units.

Harata and Uedaira[10] have recently measured the ICD spectra of β-$\mathrm{CD_x}$ complexes with naphthalene derivatives and determined the structure of the β-$\mathrm{CD_x}$ complexes on the basis of the calculation of the rotational strengths by the Kirkwood-Tinoco equation.[11] Yamaguchi *et al.* have studied the ICD spectra of β-$\mathrm{CD_x}$ complexes with 2-hydroxytropone[12] and azulene,[13] and have discussed the direction of the electronic transition moment of the guest molecules.

In the previous paper,[14] we have reported the ICD spectra of β-$\mathrm{CD_x}$ inclusion complexes with mono-substituted and para-disubstituted benzenes in aqueous solution, and have shown that these β-$\mathrm{CD_x}$ complexes favor the axial inclusion in which the long axis of the substituted benzenes is parallel to the axis of the β-$\mathrm{CD_x}$ cavity. We can estimate the orientation of the guest molecule from the comparison between the observed and calculated rotational strengths, when the direction of the electric transition dipole moment is known.

In the present article we report the ICD spectra of the β-$\mathrm{CD_x}$ complexes with *o*-, *m*-, and *p*-disubstituted benzenes in aqueous solution, and predict the orientation direction of the guest molecules in these inclusion complexes by the comparison between the observed rotational strengths of each ICD band and the values calculated by using the Kirkwood-Tinoco equation. In the manner of inclusion, β-$\mathrm{CD_x}$ complexes with *o*- and *m*-disubstituted benzenes cannot be classified into either the so-called axial or the equatorial inclusion, since the long- and/or short-axis of these molecules cannot be defined unequivocally.

Experimental

β-$\mathrm{CD_x}$ and homo- and hetero-disubstituted benzenes were obtained commercially. β-$\mathrm{CD_x}$, *o*-nitroaniline, and *o*-, *p*-phenylenediamines were purified by the recrystallization from aqueous solutions. Pyrocatechol and hydroquinone were recrystallized from benzene. *m*-Nitroaniline, *p*-nitroaniline, resorcinol, and *m*-phenylenediamine were recrystallized from ethanol, methanol, chloroform, and ether, respectively.

An inclusion complex was prepared by mixing β-$\mathrm{CD_x}$ and the corresponding disubstituted benzene using the following solvents: an aqueous solution for nitroanilines, 0.1 M†† aqueous HCl for benzenediols, 1.0×10^{-3} M or 1.0×10^{-5} M aqueous KOH for phenylenediamines.

The circular dichroism and absorption spectra were measured at room temperature using a JASCO J-500 circular dichrograph with a J-DP 500 data-processor and a Hitachi EPS-3T recording spectrophotometer, respectively.

In particular, an appropriate amount of nitrogen was bubbled through each solution of the β-$\mathrm{CD_x}$–phenylenediamine systems before the measurements, since phenylenediamines were easily oxidized by dissolved oxygen.

The experimental values of the dipole strengths, D, and the rotational strengths, R, of disubstituted benzenes were estimated in the same way as was used in the previous work.[14]

In the present paper, molar ellipticity was normalized by the concentration of the guest molecule.

Theoretical

The theoretical rotational strength of the transition from the ground state 0 to the excited state a in benzene derivative (i), R_{i0a}, was calculated by the following expression developed by Kirkwood and Tinoco:

$$R_{\mathrm{i0a}} = \pi\tilde{\nu}_{\mathrm{ai}}\mu_{\mathrm{i0a}}^{2}\sum_{\mathrm{j}}\frac{\tilde{\nu}_{\mathrm{bj}}^{2}(\alpha_{33}-\alpha_{11})_{\mathrm{j}}(\mathrm{GF})_{\mathrm{ij}}}{\tilde{\nu}_{\mathrm{bj}}^{2}-\tilde{\nu}_{\mathrm{ai}}^{2}}, \tag{1}$$

---

† Present address: Research Institute for Polymers and Textiles, 1-1-4, Yatabe-Higashi, Tsukuba, Ibaraki 305.

†† 1 M=1 mol/dm³.

$$(\mathrm{GF})_{ij} = \frac{1}{r_{ij}^{3}}\left[\hat{e}_i \cdot \hat{e}_j - \frac{3(\hat{e}_i \cdot \vec{r}_{ij})(\hat{e}_j \cdot {}_i\vec{r}_j)}{r_{ij}^{2}}\right]\hat{e}_i \times \hat{e}_j \vec{r}_{ij}. \quad (2)$$

Here $\boldsymbol{e}_j$ is the unit vector in the direction of the symmetry axis of the bond (j) in β-CD_x; $\boldsymbol{e}_i$ is the unit vector in the direction of the electric transition dipole moment, $\boldsymbol{\mu}_{ioa}$, of the transition from the ground state 0 to the excited state a in the disubstituted benzene, and $\tilde{\nu}_{ai}$ is its wave number; α_{33} and α_{11} are bond polarizabilities at zero frequency parallel and perpendicular, respectively, to the symmetry axis of the bond in β-CD_x; $\vec{r}_{ij}$ is the vector pointing from the center of benzene derivatives to each bond in β-CD_x; and $\tilde{\nu}_{bj}$ is the averaged wave number of the electronic transitions of the bond in β-CD_x.

In this calculation, $\tilde{\nu}_{bj}$ is approximated by a wave number midway between the first absorption band in the bond of β-CD_x and its ionization potential. We

TABLE 1. OBSERVED AND CALCULATED ENERGY AND DIPOLE STRENGTH (D) OF THE ELECTRONIC TRANSITIONS OF DISUBSTITUTED BENZENES

Disubstituted benzenes	Experiment $\tilde{\nu}\times10^{-3}$ cm^{-1}	Experiment D Debye^2	Calculation $\tilde{\nu}\times10^{-3}$ cm^{-1}	Calculation D Debye^2	Assignment and Φ	
	a)					
Pyrocatechol	36.3	1.84			A_1	
	46.5	6.39			B_2	
	a)					
Resorcinol	36.6	1.34	f)		B_2	
	46.5		45.2	1.75	A_1	
	a)					
Hydroquinone	34.6	2.35			B_{2u}	
	45.3	4.35			B_{1u}	
	b)					
o-Phenylenediamine	34.6	3.35			A_1	
	43.1	8.53			B_2	
	b)					
m-Phenylenediamine	34.6	2.04			B_2	
	42.0	7.53e)			A_1	
	c)					
p-Phenylenediamine	32.8	2.59			B_{2u}	
	41.5	13.61			B_{1u}	
	d)		f)			
o-Nitroaniline	24.3	9.48	27.6	19.15	A′	(−38.9°)
	35.3	7.64	38.5	5.83	A′	(−3.6°)
			42.5	8.27	A′	(20.8°)
	44.7	27.09	44.6	28.69	A′	(29.3°)
	d)		f)			
m-Nitroaniline	27.9	3.34e)	27.7	8.29	A′	(48.0°)
	35.7	4.44e)	38.1	6.64	A′	(36.6°)
	40.2e)	6.95e)	41.4	30.82	A′	(−19.3°)
	44.3	19.66e)	44.8	22.10	A′	(−44.1°)
	d)		f)			
p-Nitroaniline	26.3	27.51	32.6	18.90	A_1 (CT)	
			34.7	0.24	B_2	
	44.1	14.52	43.1	4.10	B_2 (CT)	
			48.7	0.15	A_1	

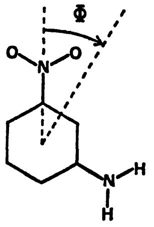

a) In 0.1 M aqueous HCl. b) In 1.0×10^{-5} M aqueous KOH. c) In 1.0×10^{-3} M aqueous KOH. d) In aqueous solution. e) Obtained by a curve fitting method. f) Obtained by the PPP SCF-MO calculation. A. Kaito, A. Tajiri, and M. Hatano, *Bull. Chem. Soc. Jpn.*, **49**, 2207 (1976).

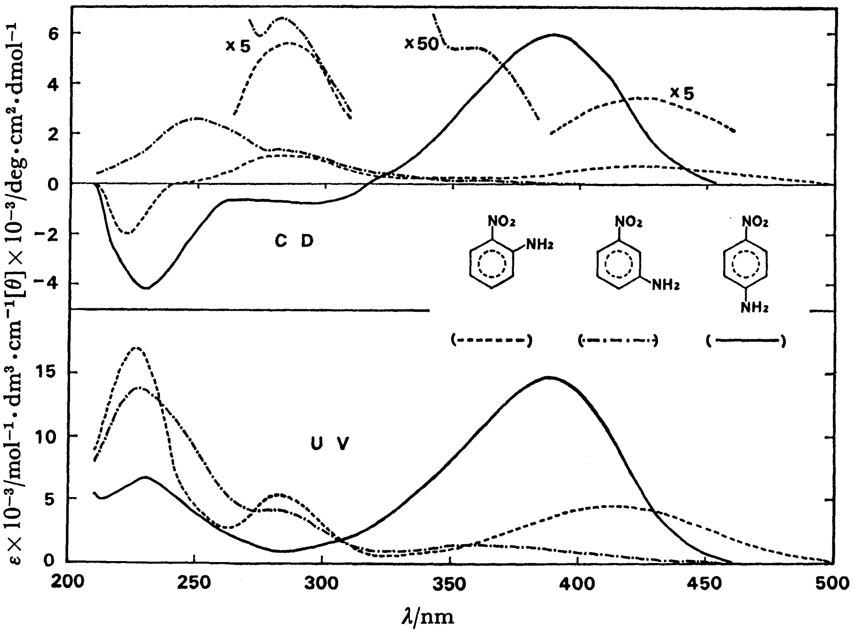

Fig. 1. CD (upper) and UV absorption (lower) spectra of the β-CD$_x$ complexes with *o*-, *m*-, and *p*-nitroanilines in aqueous solution at room temperature.
Broken line: β-CD$_x$ (1.11×10^{-2} M) +*o*-nitroaniline (3.24×10^{-4} M), dotted broken line: β-CD$_x$ (1.29×10^{-2} M)+*m*-nitroaniline (1.12×10^{-3} M), solid line: β-CD$_x$ (1.47×10^{-2} M)+*p*-nitroaniline (8.41×10^{-5} M).

used the values of $(\alpha_{33}-\alpha_{11})$ and $\tilde{\nu}_{bj}$ for each bond as listed in our previous paper.[14]

Table 1 shows the observed and calculated wave number, $\tilde{\nu}$, and the dipole strength, D, of the electronic transitions of disubstituted benzenes, along with the assignment of each electronic transition.[15] The calculated values in this table were obtained by the Pariser-Parr-Pople (PPP) SCF-MO method. The directions of the electric transition moment in homo-disubstituted benzenes were available easily from the results of the perturbation theory formulas by Petruska.[16] The experimental values in Table 1 were used for the calculation of rotational strength except in the case of the $^1A_1\leftarrow{}^1A_1$ transition of resorcinol, the third $\pi^*\leftarrow\pi$ transition of *o*-nitroaniline, and the $^1B_2\leftarrow{}^1A_1$ and $^1A_1\leftarrow{}^1A_1$ transitions of *p*-nitroaniline.

In the present calculation, the determination of the coordinates of β-CD$_x$ was carried out in the manner used in our previous paper.[14]

Results and Discussion

Figures 1—3 show the CD (upper) and UV (lower) spectra of the β-CD$_x$ complexes with *o*-, *m*-, and *p*-disubstituted benzenes. ICD bands were observed at absorption frequencies of achiral benzene derivatives.

As shown in Fig. 1, the β-CD$_x$ complex with *o*-nitroaniline showed two positive and one negative ICD bands at 427, 286, and 222 nm, respectively. These ICD bands were assigned to the first $\pi^*\leftarrow\pi$, the second $\pi^*\leftarrow\pi$, and the fourth $\pi^*\leftarrow\pi$ transitions, respectively, on the basis of the results calculated by the PPP SCF-MO method in Table 1.

The β-CD$_x$–*m*-nitroaniline complex exhibited positive

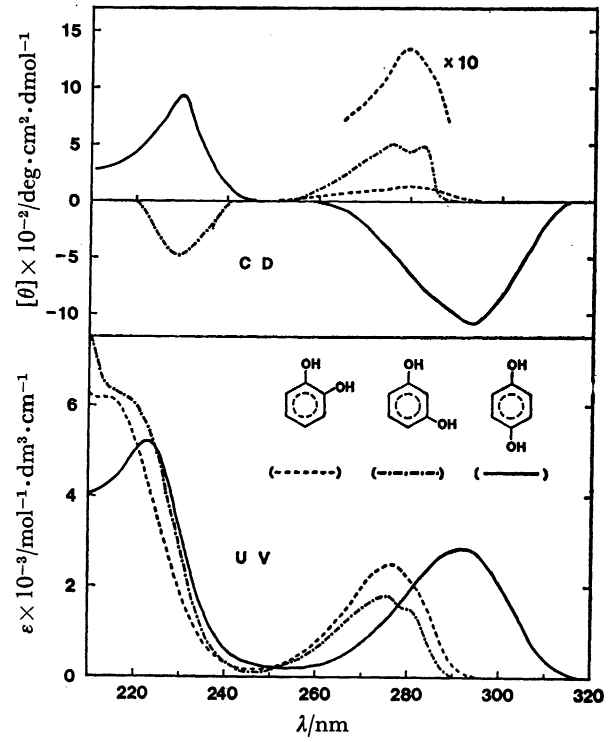

Fig. 2. CD (upper) and UV absorption (lower) spectra of the β-CD$_x$ complexes with *o*-, *m*-, and *p*-benzenediols in 0.1 M aqueous HCl at room temperature.
Broken line: β-CD$_x$ (1.17×10^{-2} M)+pyrocatechol (5.10×10^{-4} M), dotted broken line: β-CD$_x$ (1.43×10^{-2} M)+resorcinol (5.90×10^{-4} M), solid line: β-CD$_x$ (1.11×10^{-2} M)+hydroquinone (2.77×10^{-4} M).

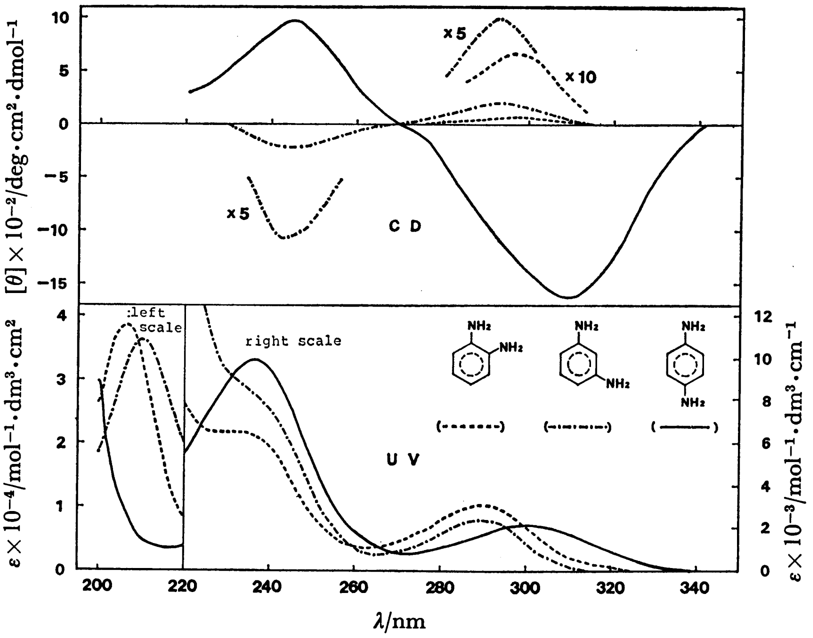

Fig. 3. CD (upper) and UV absorption (lower) spectra of the β-CD_x complexes with *o*-, *m*-, and *p*-phenylenediamines in aqueous KOH at room temperature. Broken line: β-CD_x (1.44×10^{-2} M)+*o*-phenylenediamine (1.83×10^{-4} M) (pH 7.5), dotted broken line; β-CD_x (1.43×10^{-2} M)+*m*-phenylenediamine (1.44×10^{-4} M) (pH 7.2), solid line; β-CD_x (1.45×10^{-2} M)+*p*-phenylenediamine (6.23×10^{-4} M) (pH 11.0).

ICD bands at 358, 281, and 249 nm, which are attributed to the first $\pi^*\leftarrow\pi$, the second $\pi^*\leftarrow\pi$, and the third $\pi^*\leftarrow\pi$ transitions, respectively. The lowest positive ICD band of the β-CD_x-*p*-nitroaniline complex observed at 390 nm was assigned to the $^1A_1\leftarrow{}^1A_1$ transition, and the two negative ICD bands found at 296 and 230 nm were attributed to the $^1B_2\leftarrow{}^1A_1$ transitions.

On the other hand, as seen in Fig. 2, the β-CD_x complex with pyrocatechol showed only a positive ICD band at 279 nm, originating from the $^1A_1\leftarrow{}^1A_1$ transition. But the ICD band derived from the $^1B_2\leftarrow{}^1A_1$ transition was not observed in the shorter wavelength region. The β-CD_x–resorcinol complex exhibited positive and negative ICD bands at 276 and 229 nm. These ICD bands were assigned to the $^1B_2\leftarrow{}^1A_1$ and $^1A_1\leftarrow{}^1A_1$ transitions, respectively. The β-CD_x–hydroquinone complex showed a negative ICD band attributed to the $^1B_{2u}\leftarrow{}^1A_g$ at 294 nm and exhibited a positive ICD band derived from the $^1B_{1u}\leftarrow{}^1A_g$ transition at 230 nm.

As shown in Fig. 3, each sign of the ICD spectra of the β-CD_x complexes with *o*-, *m*-, and *p*-phenylenediamines is in agreement with that of the β-CD_x complexes with *o*-, *m*-, and *p*-benzenediols (Fig. 2).

In our previous work,[14] we discussed the orientation of the guest molecule which is included in the cavity of the β-CD_x by the comparison of observed and calculated rotational strengths. One might conclude from the results of the investigation that the favorable orientation of the guest molecule about the axis of β-CD_x cavity (the Z-axis) can be estimated when the direction of the electric transition dipole moment is known. It was shown that the calculated rotational strengths were

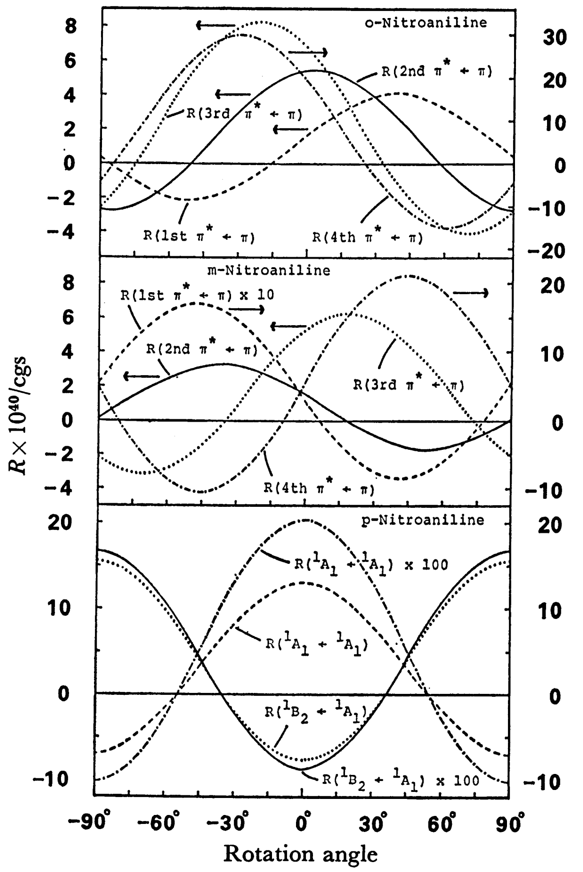

Fig. 4. The dependence of the calculated rotational strengths of the β-CD_x–nitroanilines complexes on the rotation angle in the X-Z plane.

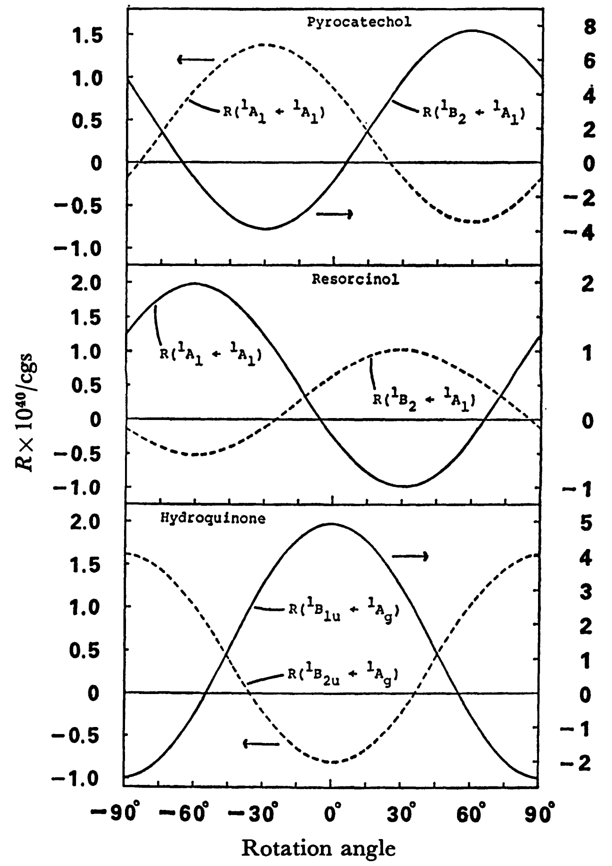

Fig. 5. The dependence of the calculated rotational strengths of β-CD$_x$–benzenediols complexes on the rotation angle in the X-Z plane.

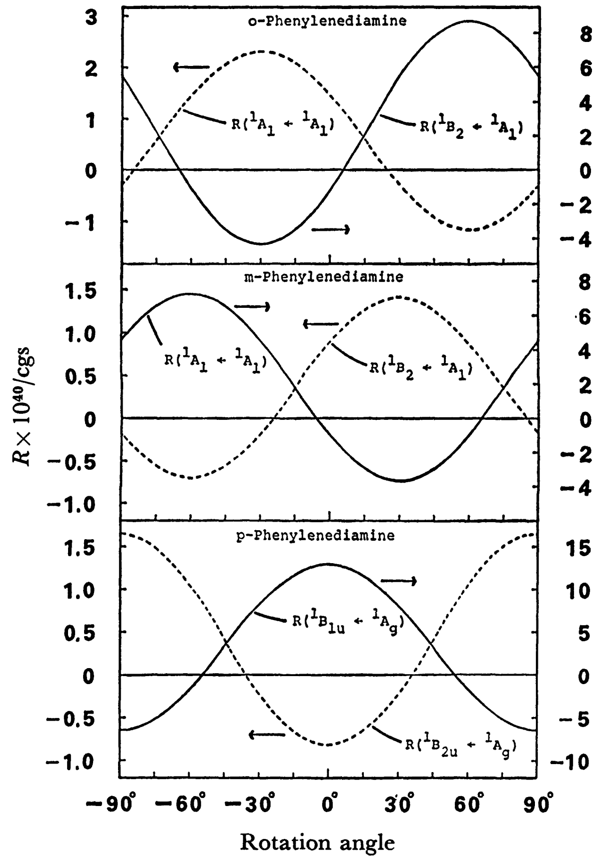

Fig. 6. The dependence of the calculated rotational strengths of β-CD$_x$–phenylenediamines complexes on the rotation angle in the X-Z plane.

very sensitive to the electric transition moment of the guest molecule and the orientation of the guest molecule in the β-CD$_x$ cavity. So, in the present work, we studied how to fit the calculated rotational strengths with the observed values obtained from ICD spectra by changing the direction of the guest molecule in the X-Z plane.

Figures 4—6 show the dependence of the calculated rotational strengths of the β-CD$_x$ complexes with disubstituted benzenes on the orientation of the guest molecule in the X-Z plane. In Fig. 4 the rotation angle on the abscissa indicates the inclined angle of the vector pointing from the center of nitroanilines to the nitro group with respect to the Z-axis (the axis of β-CD$_x$ torus). Similarly, in Figs. 5 and 6 the abscissa represents the inclined angle of the vector pointing from the center of homo-disubstituted benzenes to one of the substituents with respect to the Z-axis.

The comparison of the observed rotational strengths obtained from ICD spectra with the values calculated for the favorable orientation is listed in Table 2.

As shown at the top of Fig. 4, the calculated rotational strengths of the β-CD$_x$–*o*-nitroaniline complex in which the nitro group of *o*-nitroaniline inclines to the Z-axis by about 32° to 33° are in good agreement with the experimental values. On the other hand, in the case of *m*-nitroaniline the calculated values with an inclined angle of about −10° to −11° are compatible with the observed values. The calculated values of the β-CD$_x$–*p*-nitroaniline complex agree well with the experimental data when the nitro group of *p*-nitroaniline has an inclination with respect to the Z-axis in the range of about 0° to ±20° (bottom of Fig. 4). The experimental rotational strengths of the β-CD$_x$ complex with pyrocatechol are well reproduced by the calculation when the rotation angle is about 5° (top of Fig. 5). The calculated results of the β-CD$_x$–resorcinol complex are in accord with the observed values in the range of rotation angle from 0° to 30° (middle of Fig. 5). In this case, the orientation with roration angle 0° is equivalent to that with rotation angle 60°. The theoretical values of the β-CD$_x$–hydroquinone complex in which one of hydroxyl groups is inclined in the range of about 0° to ±20° with respect to the Z-axis are consistent with the experimental data (bottom of Fig. 5).

The same rotation angle for the β-CD$_x$ complexes with *o*-, *m*-, and *p*-phenylenediamines as that for the corresponding complexes with *o*-, *m*-, and *p*-benzenediols, respectively, gives the theoretical results in agreement with the experimental data, as demonstrated in Fig. 6 and/or in Table 2. This suggests that *o*-, *m*-, and *p*-phenylenediamines are included in the β-CD$_x$ cavity in a same way that *o*-, *m*-, and *p*-benzenediols, respectively, are included.

The results discussed above are summarized in Figs. 7 and 8. These figures illustrate the orientation directions of disubstituted benzenes included as guest molecules

TABLE 2. COMPARISON OF THE OBSERVED AND CALCULATED ROTATIONAL STRENGTH (R_{10a}) OF THE β-CD$_x$ COMPLEXES WITH *o*-, *m*-, AND *p*-DISUBSTITUTED BENZENES

Benzene derivative	$\lambda_{\max}$ nm		$R_{10a}\times 10^{40}$/cgs Experiment	Calculation	
				(32°)	
o-Nitroaniline	427	A′	1.00	3.98	
	286	A′	1.25	3.62	
	[235]a)	A′	—	0.40	
	222	A′	−1.01	−4.60	
				(−11°)	
m-Nitroaniline	358	A′	0.23c)	0.78	
	281	A′	0.56c)	2.33	
	249	A′	3.42c)	3.83	
	(226)b)	A′	—	0.19	
				(0°)	(20°)
p-Nitroaniline	390	A_1	9.14	13.05	10.75
	[296]a)	B_2	−0.52	−0.08	−0.06
	230	B_2	−5.37	−7.78	−5.05
	[205]a)	A_1	—	0.20	0.17
				(5°)	
Pyrocatechol	279	A_1	0.08	0.70	
	(215)b)	B_2	—	−0.05	
				(0°)	(30°)
Resorcinol	276	B_2	0.25	0.64	1.02
	229	A_1	−0.18	−0.25	−0.99
				(0°)	(20°)
Hydroquinone	294	B_{2u}	−0.72	−0.82	−0.53
	230	B_{1u}	0.52	4.94	1.72
				(5°)	
o-Phenylenediamine	297	A_1	0.04	1.18	
	(232)b)	B_2	—	−0.06	
				(0°)	(30°)
m-Phenylenediamine	293	B_2	0.12	0.89	1.42
	243	A_1	−0.14	−0.91	−3.65
				(0°)	(20°)
p-Phenylenediamine	313.5	B_{2u}	−1.46	−0.83	−0.54
	245	B_{1u}	0.86	12.89	10.63

a) Value calculated by the PPP SCF-MO method. b) UV absorption peak in the presence of β-CD$_x$.
c) Obtained by a curve fitting method.

in the cavity of β-CD$_x$. The β-CD$_x$ cavity, in both figures, was represented schematically by a pair of rectangles with oblique lines. Each dotted line in Fig. 7 indicates the direction of the transition dipole moment obtained from the PPP SCF-MO calculation, and the numbers, 1, 2, 3, and 4 designate the first $\pi^*\leftarrow\pi$, the second $\pi^*\leftarrow\pi$, the third $\pi^*\leftarrow\pi$, and the fourth $\pi^*\leftarrow\pi$ transitions of *o*- and *m*-nitroanilines, respectively. Similarly, each dotted line in Fig. 8 indicates the directions of the electric transition moments of homo-disubstituted benzenes derived from the perturbation theory formulas by Petruska.[16] In addition, the symbols (+) and (−) give the signs of the CD spectra induced by the electronic transitions of the corresponding disubstituted benzenes.

We could make no reference to the discrimination of the top side from the bottom side of β-CD$_x$, because the coulombic interaction between CD$_x$ and the guest molecule was approximated by the interaction between the distributed bond dipole of CD$_x$ and the point dipole of the guest molecule in the present calculation.

On the other hand, it seems likely from Figs. 7 and 8 that some of the substituents of the guest molecules are linked by the hydrogen bond to the hydroxyl group of β-CD$_x$, or are in van der Waals contact with the interior of the β-CD$_x$ torus. However, it appears that the conformational change in one or two of the C(5)–O(6) bonds is required for the guest-host linkage by a hydrogen bond with the primary hydroxyl group.[17]

In conclusion, the orientation of the guest molecule which is included in the β-CD$_x$ cavity seems to be confined about the axis of the β-CD$_x$ torus.

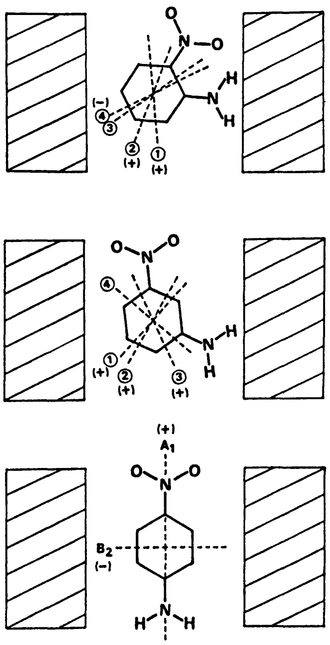

Fig. 7. The schematic drawing of the orientation of *o*-, *m*-, and *p*-nitroanilines included in the cavity of β-CD$_x$.

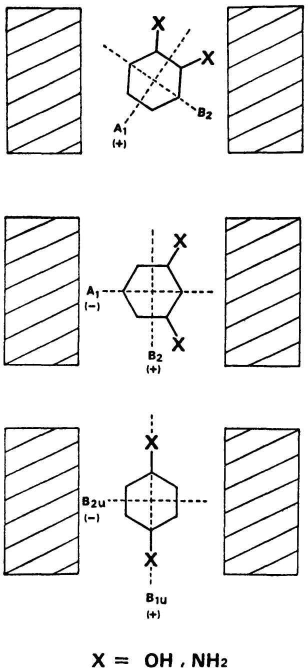

Fig. 8. The schematic drawing of the orientation of *o*-, *m*-, and *p*-homodisubstituted benzenes included in the cavity β-CD$_x$.

References

1) F. Schardinger, *Zentr. Bakt. Parasitenk.*, *II*, **29**, 188 (1911).

2) M. L. Bender and M. Komiyama, "Cyclodextrin Chemistry," Springer-Verlag, Berlin (1978).

3) F. Cramer and W. Kampe, *J. Am. Chem. Soc.*, **87**, 1115 (1965).

4) M. L. Bender, R. L. VanEtten, G. A. Clowes, and J. F. Sebastian, *J. Am. Chem. Soc.*, **88**, 2318, 2319 (1966); R. L. VanEtten, J. F. Sebastian, G. A. Clowes, and M. L. Bender, *ibid.*, **89**, 3242, 3253 (1967).

5) R. Breslow and P. Campbell, *J. Am. Chem. Soc.*, **91**, 3085 (1969).

6) I. Tabushi, K. Yamamura, K. Fujita, and H. Kawakubo, *J. Am. Chem. Soc.*, **101**, 1019 (1979).

7) R. Breslow, J. B. Doherty, G. Guillot, and C. Lipsey, *J. Am. Chem. Soc.*, **100**, 3227 (1978); R. Breslow, M. F. Czarniecki, J. Emert, and H. Hamaguchi, *ibid.*, **102**, 762 (1980).

8) A. Ueno, H. Yoshimura, R. Saka, and T. Osa, *J. Am. Chem. Soc.*, **101**, 2779 (1979).

9) I. Tabushi, Y. Kuroda, and K. Shimokawa, *J. Am. Chem. Soc.*, **101**, 4759 (1979); I. Tabushi, Y. Kuroda, and A. Mochizuki, *ibid.*, **102**, 1152 (1980).

10) K. Harata and H. Uedaira, *Bull. Chem. Soc. Jpn.*, **48**, 375 (1975).

11) I. Tinoco, Jr., *Adv. Chem. Phys.*, **4**, 113 (1962).

12) H. Yamaguchi, N. Ikeda, F. Hirayama, and K. Uekama, *Chem. Phys. Lett.*, **55**, 75 (1978).

13) N. Ikeda and H. Yamaguchi, *Chem. Phys. Lett.*, **56**, 167 (1978).

14) H. Shimizu, A. Kaito, and M. Hatano, *Bull. Chem. Soc. Jpn.*, **52**, 2678 (1979).

15) A. Kaito, A. Tajiri, and M. Hatano, *Bull. Chem. Soc. Jpn.*, **49**, 2207 (1976).

16) J. Petruska, *J. Chem. Phys.*, **34**, 1111 (1961).

17) W. Saenger, R. K. McMullan, J. Fayos, and D. Mootz, *Acta Crystallogr., Sect. B*, **30**, 2019 (1974).